

Surge-sway simulations with additional detail

by H. Alemi Ardakani & T. J. Bridges

Department of Mathematics, University of Surrey, Guildford GU2 7XH UK

— December 16, 2009 —

1 Introduction

This report is a slightly expanded version of §13 of [1], showing a wider range of contour plots and additional simulations.

2 Numerical results: coupled surge-sway motion

Surge-sway forcing is the most studied of forcing functions for 3D sloshing [2, 6, 3, 4, 5]. It is simple to implement since there is only translation and no orientation change. On the other hand, there are identifiable wave types and bifurcations that occur that make it easier for experimental and theoretical comparison. The results in this section are inspired by the theory and experiment of [3] and the 3D simulations of [5].

The prescribed surge and sway motions of the vessel are taken to be harmonic and in phase

$$q_1(t) = \varepsilon_1 \cos(\omega_1 t) \quad \text{and} \quad q_2(t) = \varepsilon_2 \cos(\omega_2 t),$$

and simulations with a range of amplitudes and frequencies will be presented.

Set the fluid and vessel geometry parameters at

$$L_1 = 0.5 \text{ m}, \quad L_2 = 0.5 \text{ m}, \quad \text{and} \quad h_0 = 0.07 \text{ m}, \quad (1)$$

giving a fluid aspect ratio of $h_0/L_1 = 0.14$, and natural frequencies

$$\omega_{mn} \approx 5.207 \sqrt{m^2 + n^2} \text{ rad/sec}.$$

The numerical parameters are taken to be

$$\Delta x = \Delta y = 0.025 \text{ m}, \quad \text{and} \quad \Delta t = 0.01 \text{ s}. \quad (2)$$

Following the strategy in the experiments of [3] and the simulations of [5], points on the vessel walls are identified and the time series at the fixed points are compared. Eight points are chosen and they are labelled *P1* through *P8* as shown in Figure 1.

For the first simulation, an almost longitudinal forcing is chosen with

$$\varepsilon_1 = 0.00035 \text{ m}, \quad \varepsilon_2 = 0.00035 \tan(5^\circ) \text{ m} \quad \text{and} \quad \omega_1 = \omega_2 = 1.03\omega_{1,0} = 5.3629 \text{ rad/sec}. \quad (3)$$

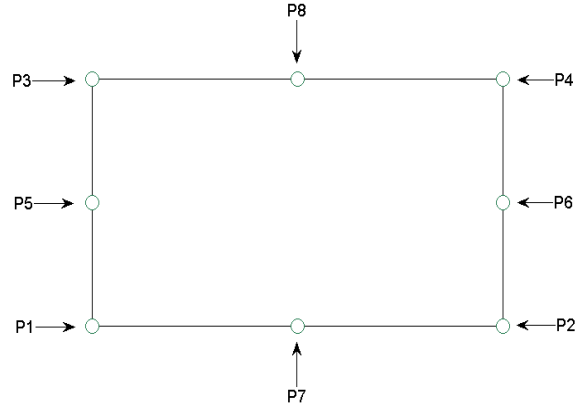


Figure 1: Location of the points P_1 to P_8 in the tank cross section.

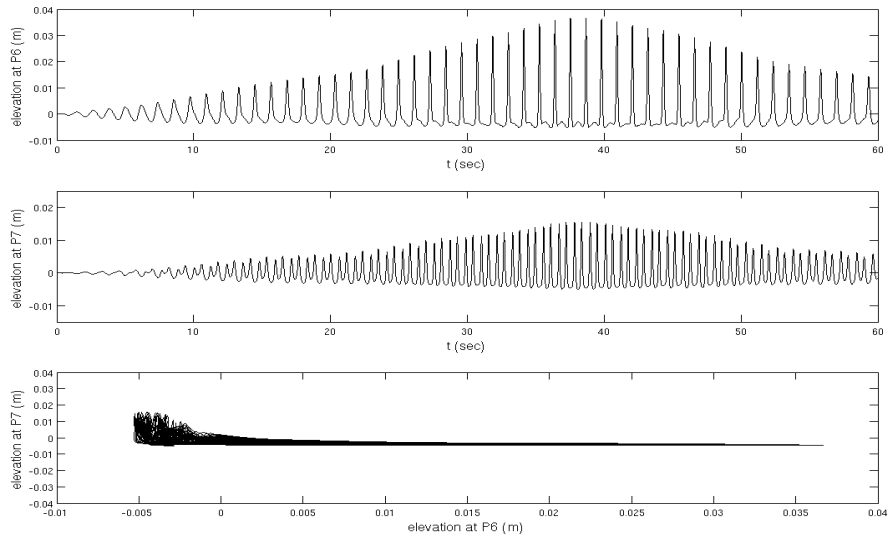


Figure 2: Time histories of the surface displacement at points P_6 and P_7 , and a parametric graph of the pair (P_6, P_7) .

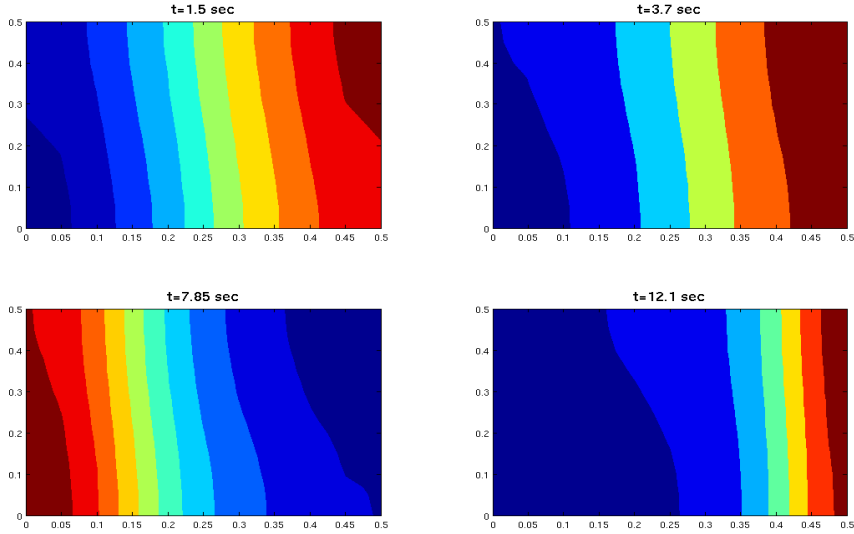


Figure 3: Contour plots of the surface profile associated with the forcing (3) at a sequence of times.

The time histories of the surface displacements at points P_6 and P_7 are depicted in Figure 2. A parametric graph, showing wave elevation at P_7 versus wave elevation at P_6 , is also depicted in Figure 2. According to the theory of [3] this type of parametric graph indicates the presence of planar waves in the tank (compare Figure 2 with Figure 15(c) in [3]). The planar nature of these waves is confirmed by the contour plots of surface profile shown at a sequence of times in Figures 3–6.

[3] solve the linearized version of the governing equations (equation (2.1) on page 7 of their paper) in terms of velocity potential and as is shown in Figure 15 of their paper the theory predicts a straight line showing the presence of planar waves under longitudinal forcing. The parametric graph of Figure 2 shows a horizontal interval as well. In this simulation the angle between surge and sway motions is 5° and this simulation is very close to the case of longitudinal forcing.

The reason that a small sway forcing is added to longitudinal surge forcing is to see if rotating waves are generated in the tank (see later simulations where rotating waves arise), and this simulation with the chosen input parameter data showed formation of planar waves in the tank – with, however, a small distortion in the contour plots which is because of the small amplitude (in comparison with the surge forcing) sway forcing.

When $\varepsilon_2 = 0$ the sloshing histories of surface displacements at points P_6 and P_7 and the parametric curve are shown in Figure 7. The parametric curve is almost the same as parametric curve in Figure 2. The corresponding contour plots of surface profile in Figure 6 are depicted in Figure 8 and they show a true planar structure without transverse distortion.

In [3] it is shown that diagonal forcing leads to three basic types of steady-state solutions for the linearized version of the governing equations (equation (2.1) on page

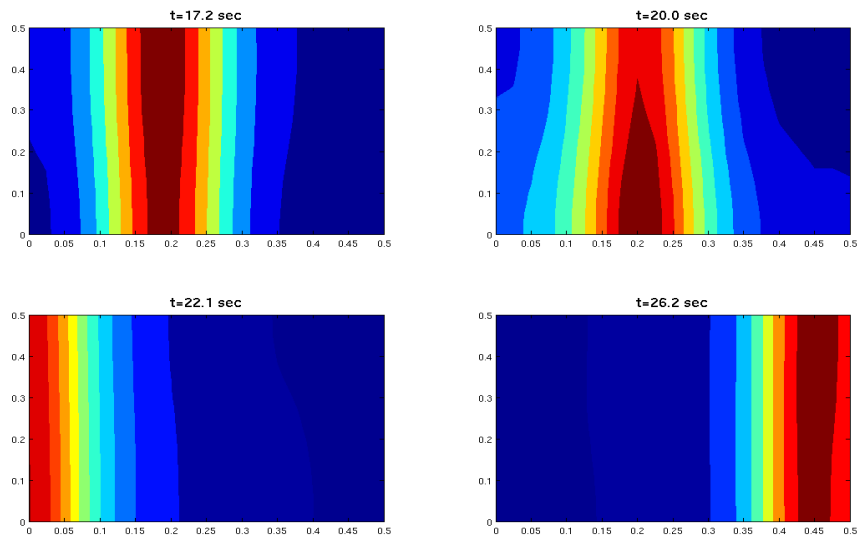


Figure 4: Contour plots of surface profile associated with the forcing (3) at a sequence of times: continued.

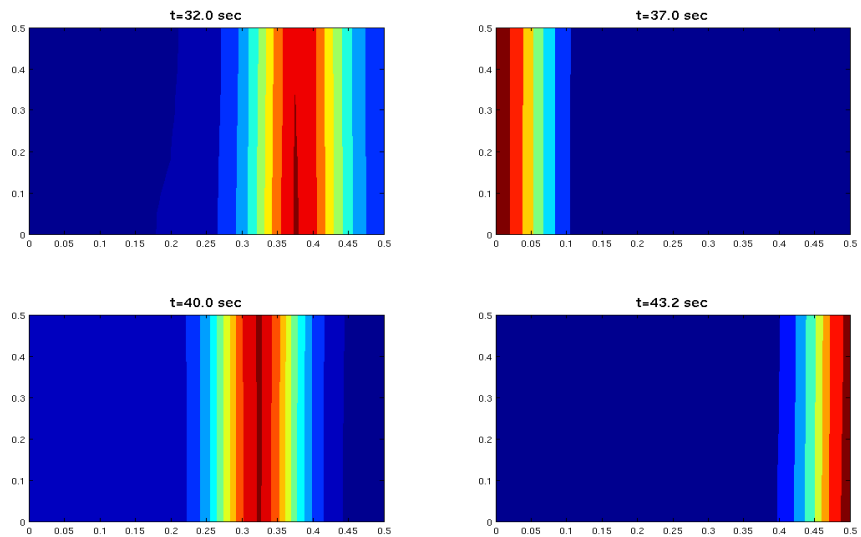


Figure 5: Contour plots of surface profile associated with the forcing (3) at a sequence of times: continued.

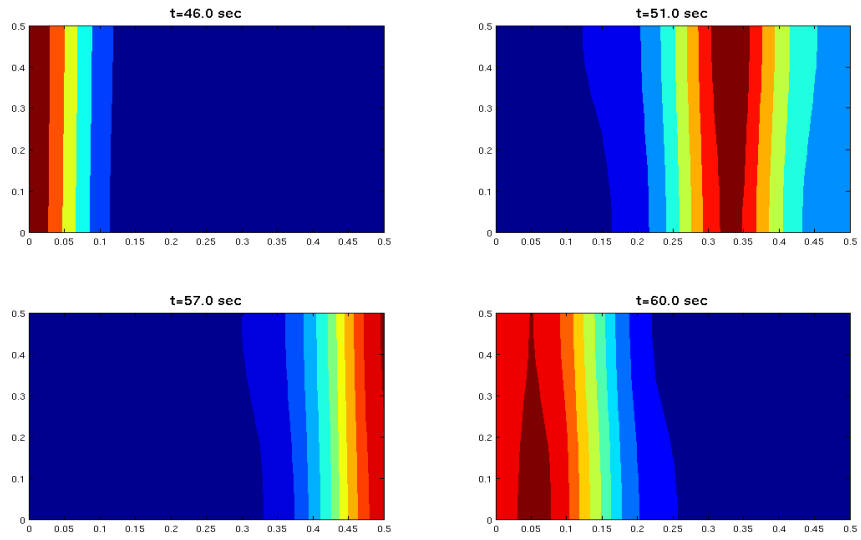


Figure 6: Contour plots of surface profile associated with the forcing (3) at a sequence of times: continued.

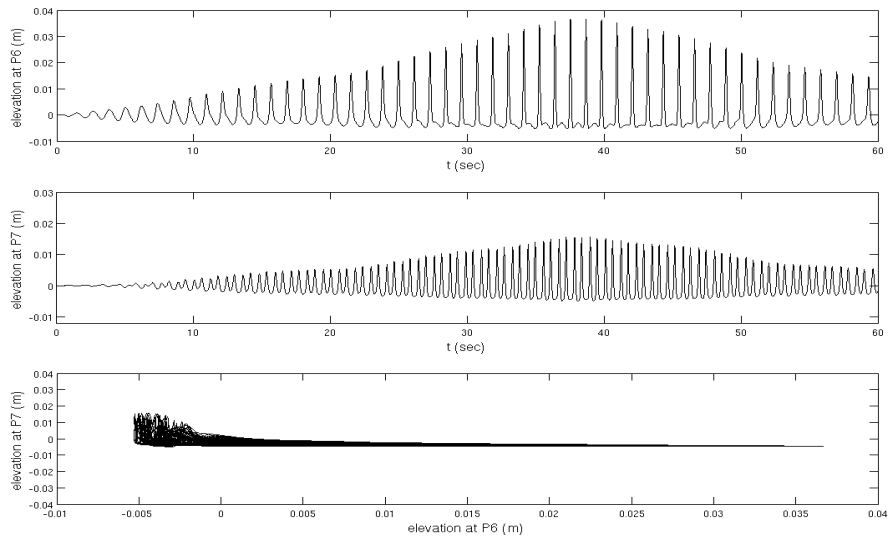


Figure 7: Time histories of the surface displacement at points P_6 and P_7 , and a parametric graph of the pair (P_6, P_7) when $\varepsilon_2 = 0$.

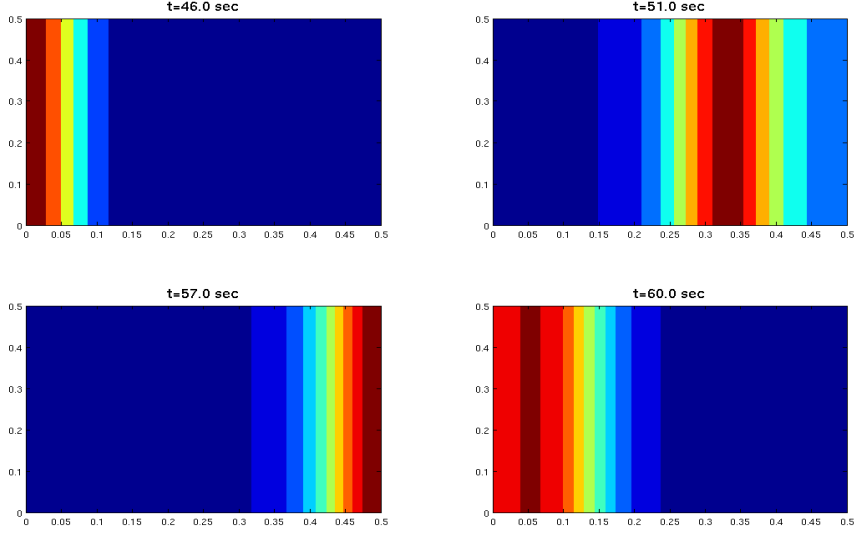


Figure 8: Contour plots of surface profile at different times when $\varepsilon_2 = 0$.

7 of their paper). Diagonal waves (equation (3.30) on page 22), square-like waves (equation (3.31) on page 22) and swirling waves (equation (3.32) page 22). Diagonal and square-like waves have a very similar formulation.

Consider the case of diagonal forcing. The parameters (1)-(2) remain the same, and the forcing function parameters are changed to

$$\varepsilon_1 = 0.002 m, \quad \varepsilon_2 = 0.002 m, \quad \text{and} \quad \omega_1 = \omega_2 = 1.4 \omega_{1,0} = 7.2893 \text{ rad/sec}. \quad (4)$$

The time histories of the surface displacement at points P_6 and P_7 and the parametric curve of the pair are shown in Figure 9. Contour plots of the surface profile at a sequence times are depicted in Figure 10. The parametric graph in Figure 9 now has a non-trivial slope. According to the theory of [3] this type parametric graph indicates of square-like waves in the tank. Square-like wave corresponds to a nearly diagonal standing wave (see the last few sentences of page 17 of [3]). The structure of a square-like wave is also seen in Figures 7(b), 8(b) and 9(b) of [5].

Consider another case of diagonal forcing with a frequency below the natural frequency. The parameters (1)-(2) remain the same, and the forcing function parameters are changed to

$$\varepsilon_1 = 0.001 m, \quad \varepsilon_2 = 0.001 m, \quad \text{and} \quad \omega_1 = \omega_2 = 0.9 \omega_{1,0} = 4.6860 \text{ rad/sec}. \quad (5)$$

The time histories of the surface displacement at points P_6 and P_7 and the parametric curve associated with the pair are shown in Figure 11. According to the theory of [3] the parametric graph of Figure 11 shows the presence of swirling waves in the tank as it has a circular pattern. This structure is also seen in Figure 12 of [5] where it is identified as a swirling wave. The swirling wave structure is confirmed in contour plots of the surface profile at different values of time in Figures 12 and 13.

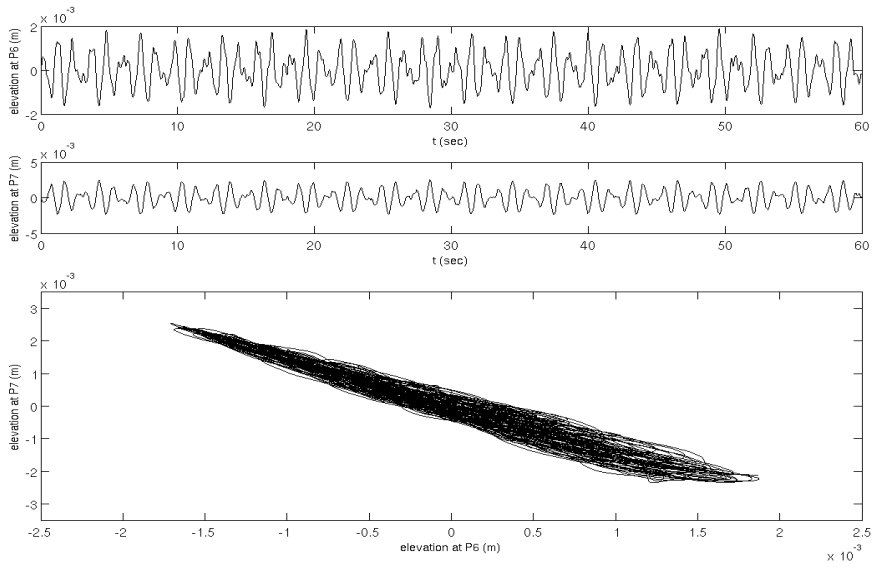


Figure 9: Time histories of the surface displacements at points P_6 and P_7 , and a parametric graph of the pair (P_6, P_7) .

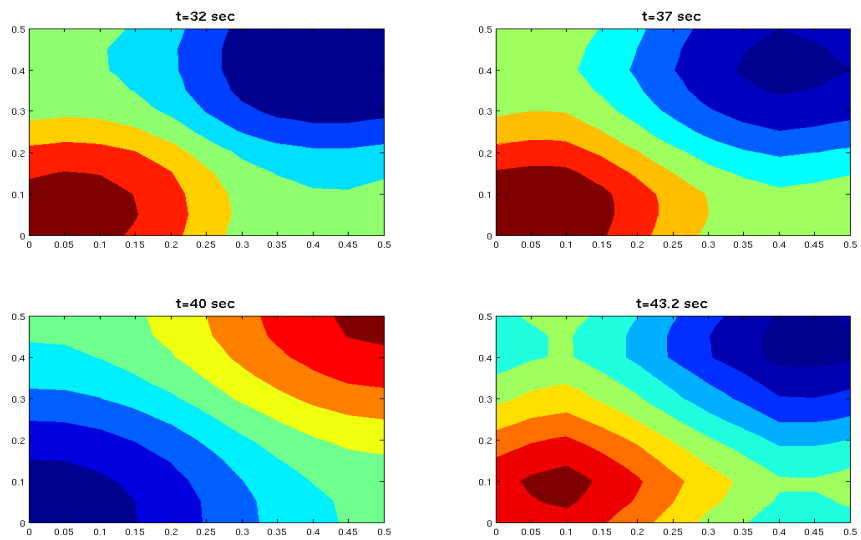


Figure 10: Contour plots of surface profile at a sequence of times associated with the forcing (4).

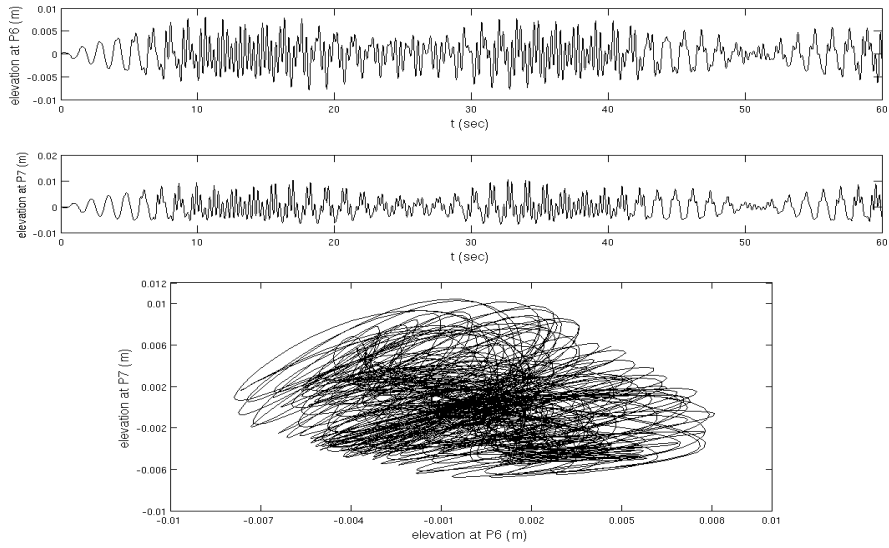


Figure 11: Time histories of the surface displacement at points P_6 and P_7 , and a parametric graph of the pair (P_6, P_7) .

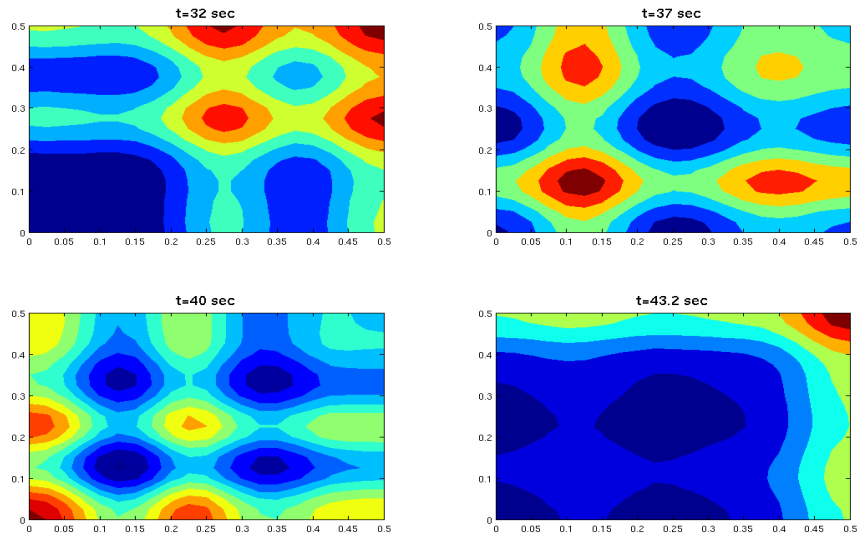


Figure 12: Contour plots of surface profile at different times associated with the forcing (5).

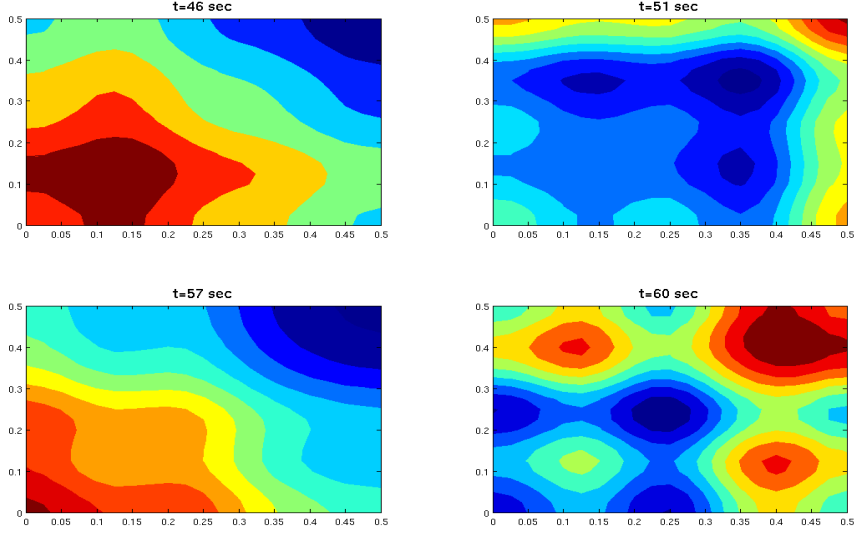


Figure 13: Contour plots of surface profile at different times associated with the forcing (5): continued.

Consider another case of diagonal forcing with a frequency well below the natural frequency. The parameters (1)-(2) remain the same, and the forcing function parameters are changed to

$$\varepsilon_1 = 0.008 \text{ m}, \quad \varepsilon_2 = 0.008 \text{ m}, \quad \text{and} \quad \omega_1 = \omega_2 = 0.35 \omega_{1,0} = 1.8223 \text{ rad/sec}. \quad (6)$$

The time histories of the surface displacement at points P_6 and P_7 and the parametric curve are shown in Figure 14. The parametric graph shows the presence of square-like (or diagonal) waves in the tank. Contour plots of the surface profile at different values of time are depicted in Figure 15.

2.1 Surge-sway forcing with a phase shift

By taking the surge and sway forcing functions to be out of phase, a clear example of a swirling wave emerges. Consider the case of diagonal forcing with the surge and sway 90° out of phase

$$q_1(t) = \varepsilon_1 \cos(\omega_1 t) \quad \text{and} \quad q_2(t) = \varepsilon_2 \sin(\omega_2 t).$$

The parameters (1)-(2) remain the same, and the forcing function parameters are taken to be

$$\varepsilon_1 = 0.00012 \text{ m}, \quad \varepsilon_2 = 0.00012 \text{ m}, \quad \text{and} \quad \omega_1 = \omega_2 = 0.99 \omega_{1,0} = 5.1546 \text{ rad/sec}. \quad (7)$$

The time histories of the surface displacement at points P_6 and P_7 and their parametric curve are shown in Figures 16 and 17 respectively. Figures 18 and 19 show the

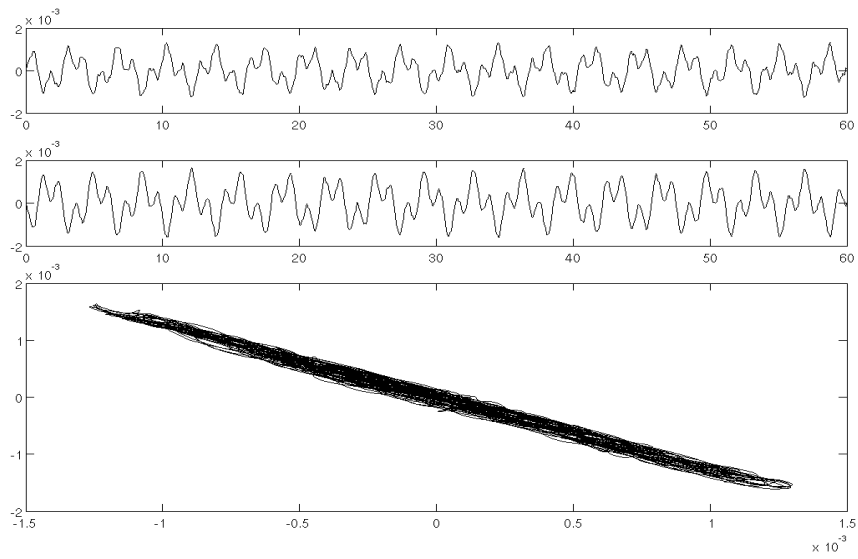


Figure 14: Time histories of the surface displacement at points P_6 and P_7 , and a parametric graph of the pair (P_6, P_7) .

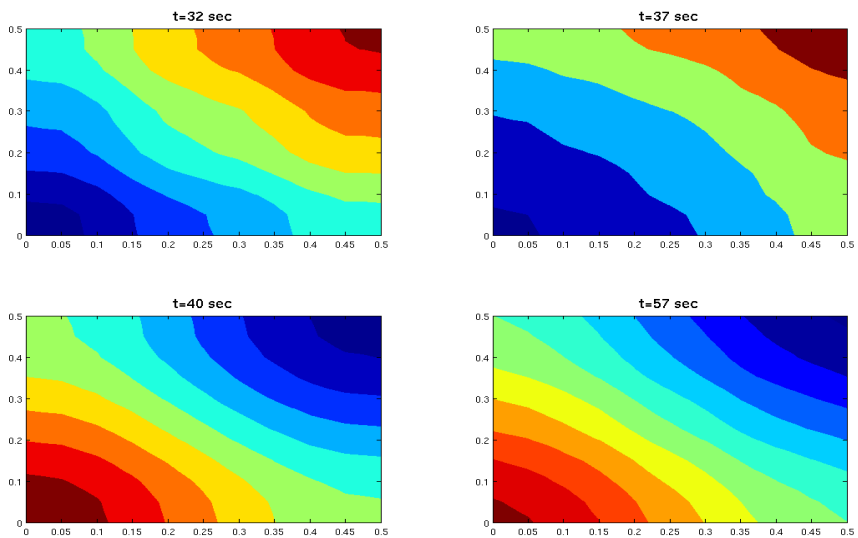


Figure 15: Contour plots of surface profile at different times associated with the forcing (6).

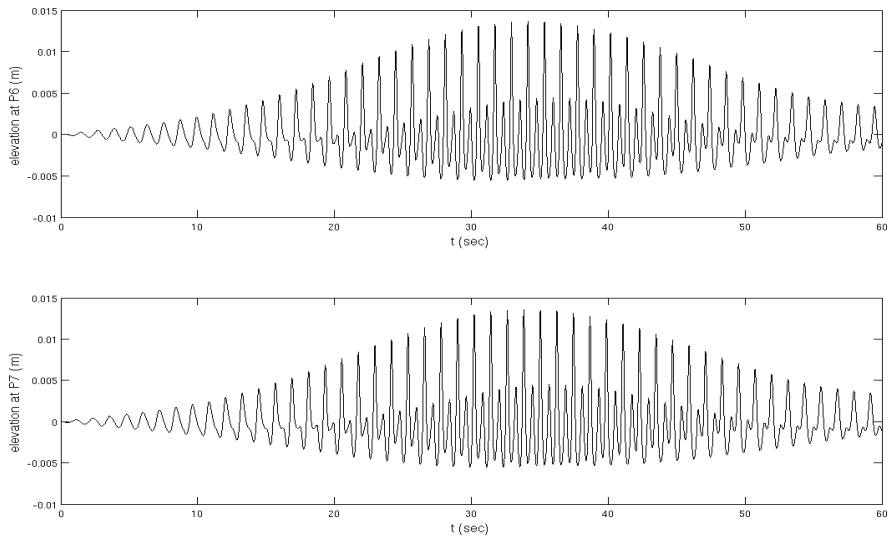


Figure 16: Time histories of surface displacements at points P_6 and P_7 associated with the out-of-phase forcing (7).

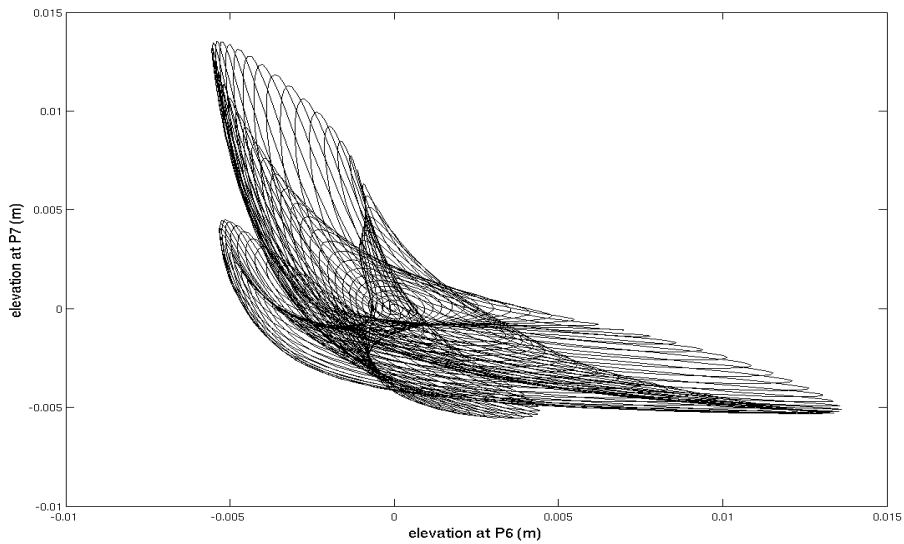


Figure 17: Parametric graph of the pair (P_6, P_7) associated with the out-of-phase forcing (7).

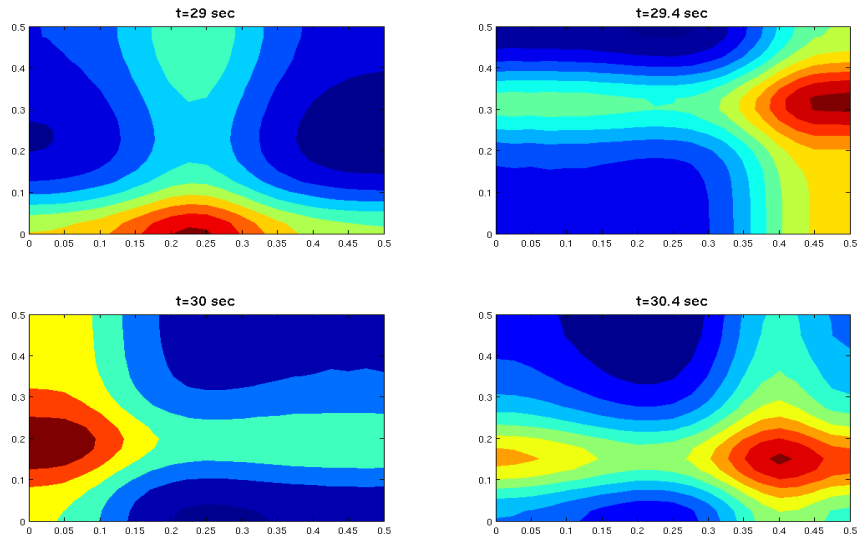


Figure 18: Contour plots of surface profile at different times associated with the out-of-phase forcing (7).

contour plots of surface profile at a sequence of times showing the propagation of a counterclockwise swirling wave along the tank walls. Another way of viewing this swirling wave is to use surface plots and they are shown in Figures 20 and 21. These surface plots agree qualitatively with the surface plots of a swirling wave in Figure 11 of [5].

References

- [1] ALEMI ARDAKANI, H. & BRIDGES, T.J. 2009 Shallow water sloshing in rotating vessels. Part 2. three-dimensional flowfield. *Preprint*.
- [2] CHEN, Y. G., DJIDJELI, K. & PRICE, W. G. 2009 Numerical simulation of liquid sloshing phenomena in partially filled containers. *Computers & Fluids* **38**, 830–842.
- [3] FALTINSEN, O. M., ROGNEBAKKE, O. F. & TIMOKHA, A. N. 2003 Resonant three-dimensional nonlinear sloshing in a square basin. *J. Fluid Mech.* **487**, 1–42.
- [4] LIU, D. & LIN, P. 2008 A numerical study of three-dimensional liquid sloshing in tanks. *J. Comp. Phys.* **227**, 3921–3939.
- [5] WU, C.-H. & CHEN, B.-F. 2009 Sloshing waves and resonance modes of fluid in a 3D tank by a time-independent finite difference method. *Ocean Eng.* **36**, 500–510.

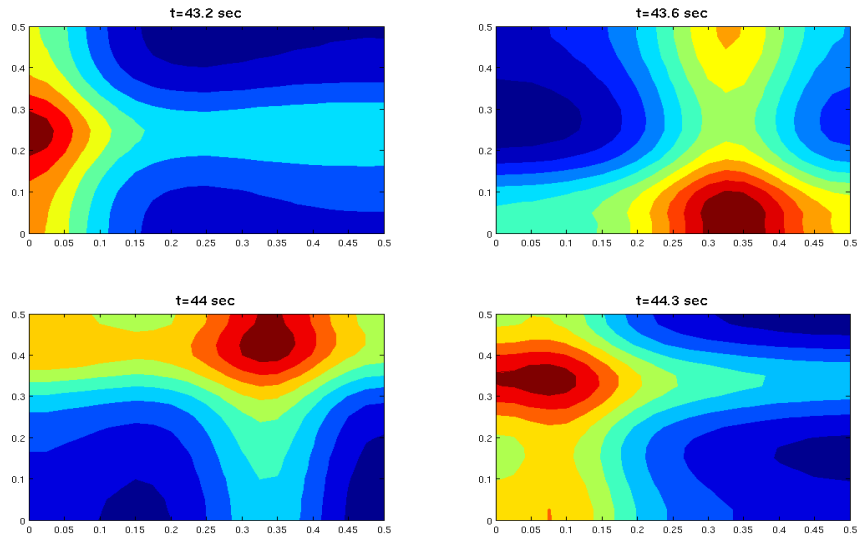


Figure 19: Contour plots of surface profile at different times associated with the out-of-phase forcing (7): continued.

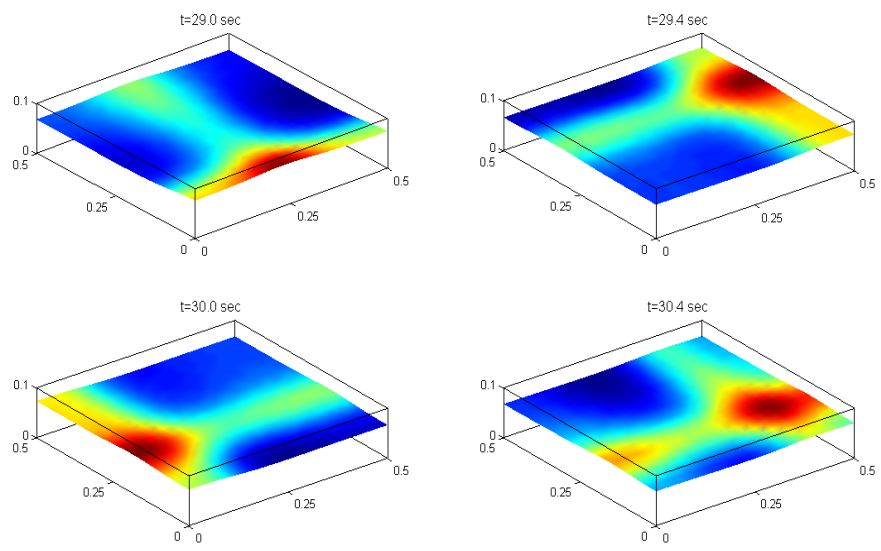


Figure 20: Surface plots of surface profile at different times associated with the out-of-phase forcing (7).

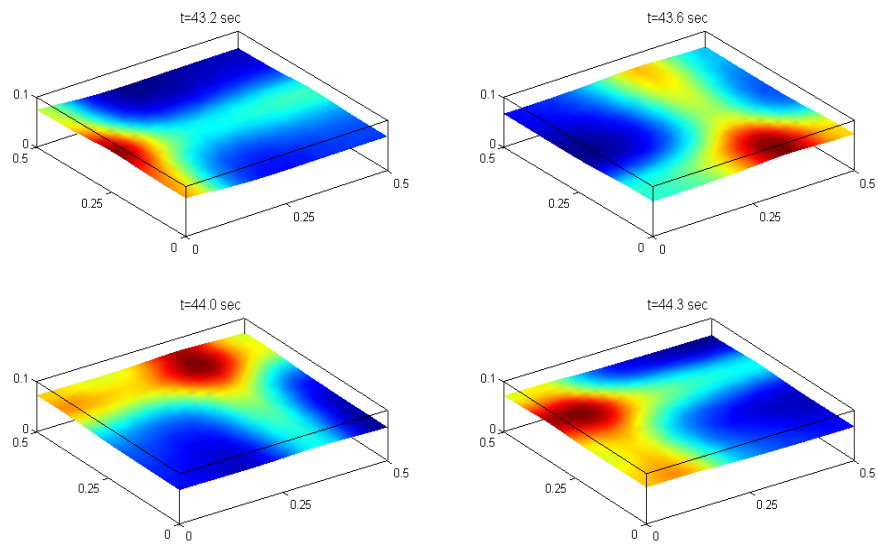


Figure 21: Surface plots of surface profile at different times associated with the out-of-phase forcing (7): continued.

- [6] WU, G. S., MA, Q. W. & EATOCK TAYLOR, R. 1998 Numerical simulation of sloshing waves in a 3D tank based on a finite element method. *Appl. Ocean Res.* **20**, 337–355.